Pergamon

PII: S0038-092X(96)00137-5

Solar Energy Vol. 57, No. 6, pp. 421–432, 1996

0038-092X/96 $15.00 + 0.00

A SIMPLE MODEL FOR PV MODULE REFLECTION LOSSES UNDER FIELD CONDITIONS

E. A. SJERPS-KOOMEN,† E. A. ALSEMA‡ and W. C. TURKENBURG‡
Department of Science, Technology & Society, Utrecht University, Padualaan 14, NL-3584CH Utrecht, The Netherlands

(Received 29 December 1995; revised version accepted 19 September 1996)
(Communicated by Gerard Wrixon)

Abstract—PV module power ratings are determined at standard test conditions, which require perpendicular incident light. Under field conditions larger incidence angles occur, resulting in higher reflection losses than accounted for in the nominal power rating. In this article we will present a model to take these losses into account, and discuss some results for practical situations. From our model we conclude that the reflection losses relative to STC are determined mainly by the air–glass interface. Limited validation assuming certain spectral losses showed a rough correspondence between calculated reflection losses and experimental values on a yearly averaged basis (1.2% difference between model and experiment). Model calculations show that for modules faced towards the equator, and with a tilt angle equal to the latitude, yearly reflection losses relative to STC are about 3%. For this tilt and orientation, the losses seem to be only slightly dependent on the geographical latitude of the location. Tilt, orientation and seasonal dependence are significant. For vertically mounted PV modules (facades) near the equator the reflection losses can be quite large (up to 8%). Copyright © 1997 Elsevier Science Ltd.

1. INTRODUCTION

In the design or simulation of PV systems, the PV module energy yield is calculated in order to predict or simulate the system performance. To determine realistic energy yields, the PV module performance under field conditions should be modelled adequately. Usually datasheets from the module manufacturer are the only available source of input parameters for PV modules. At these sheets the power of the PV modules is indicated by a peak power rating. This nominal or peak power of PV modules P_{nom} (in kWp) is determined under standard test conditions (STC): i.e., (i) light with (a) irradiance 1000 W m^{-2}, (b) perpendicular incidence, and (c) standard spectrum AM1.5G; (ii) PV module temperature 25°C.

However, in the field the module output power will be different from the peak power, when conditions differ from STC. In design and simulation of PV systems, the peak power has to be corrected for these differences in order to determine realistic values for the expected energy yield.

In this article we investigate the reflection and absorption losses relative to STC, i.e., when the incidence angle differs from perpendicular incidence.

Existing detailed models for the calculation of reflection losses have been used mainly for optimisation of PV module performance under STC. Krauter and co-workers (Krauter, 1993; Krauter *et al.*, 1994) developed a complex model for the purpose of material optimisation studies under realistic operating conditions. Scheydecker *et al.* (1994) showed calculations and measurements on absolute (i.e., not relative to STC) transmission of different kinds of experimental PV module covers. A simple model to take into account reflection losses relative to STC as a function of incidence angle is the ASHRAE incidence angle modifier (Duffie and Beckman, 1991). This model, however, requires the adjustment of a parameter and is not based directly on physical properties of the PV module cover.

In contrast, "standard" irradiance models (Orgill and Hollands, 1977; Perez *et al.*, 1987; and many others) have been developed for the purpose of tilt conversion. Integration of a reflection model and an irradiance model would enable the STC rating of PV modules to be corrected for field conditions as far as reflection and absorption losses are concerned. The resulting model should be fast enough to be implemented in simulation programs for the correct

†Author to whom correspondence should be addressed.
‡ISES member.

determination of realistic energy yields, or for the calculation of the reflection losses on an hourly, monthly, or yearly basis. Recently we proposed such a model and applied it to determine the yearly reflection losses under field conditions as a function of tilt, location and season (Sjerps-Koomen and Alsema, 1995). The model has been implemented into the simulation and optimisation model for renewable energy systems SOMES (van Dijk and Alsema, 1992). Preu *et al.* (1995) reported a more detailed and possibly time-consuming model. The calculated 2–3% yearly reflection losses relative to STC for modules with tilt angles equal to the geographical latitude are significant, but smaller than the previously reported value of 7% (Schmid, 1993). In this article we describe in more detail the model we proposed in Sjerps-Koomen and Alsema (1995) and discuss results calculated with it.

Our model follows a two-step procedure: first the transmittance τ of the cover layers is calculated as a function of incidence angle Θ, and taken *relative* to that at perpendicular incidence ($\Theta = 0°$). The *absolute* transmittance for perpendicular incidence through the cover layers into the cell is already taken into account when measuring under STC. In the second step the angular distribution of the incident irradiance $G(\Theta,t)$ is calculated at a certain point in time, and the curve $\tau_{rel}(\Theta)$ of step 1 is averaged over this distribution. The resulting model for the averaged relative transmission coefficient $\bar{\tau}_{rel}$ can be used to calculate the reflection and absorption loss $\bar{r}$ relative to STC averaged over a certain time period. The steps in this calculation and the symbols used in this article are illustrated in Fig. 1.

In this article we describe the two steps of the model in Sections 2 and 3, respectively. In Section 3 we also discuss briefly the influence of the used time step in the irradiance model. Next we compare the modelled reflection losses with experimental data (Section 4), and show some calculations indicating the influence of location, tilt, orientation, and season in Section 5.

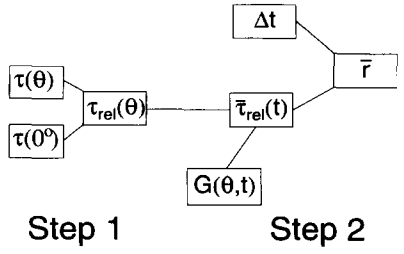

Fig. 1. Calculation scheme used in this article.

2. TRANSMITTANCE AS A FUNCTION OF INCIDENCE ANGLE

In this section we investigate models for the transmittance of crystalline Si module covers. We calculate this transmittance as a function of the incidence angle, and take it relative to the transmittance at STC.

2.1. *Slab model*

Light falling on a crystalline Si module usually has to pass a glass cover, an encapsulation layer (EVA) and an anti-reflection (AR) coating, before it can enter the silicon material of the solar cell. In each of these layers, schematically shown in Fig. 2, absorption can occur and at each interface light can be reflected.

The overall transmission coefficient from air to silicon can be defined as

$$\tau(\Theta) = G_{cell}(\Theta)/G_{mod}(\Theta) \quad (1)$$

where G_{mod} and G_{cell} are the irradiance on the module (glass) surface and at the Si wafer, respectively, at incidence angle Θ. The transmittance relative to perpendicular incidence is equal to

$$\tau_{rel}(\Theta) = \tau(\Theta)/\tau(0°) \quad (2)$$

Assuming the layers to be smooth, formulas from basic optics (Hecht, 1987) are applied to calculate the transmission from air via three slabs (glass, EVA, AR coating) to crystalline silicon. The Fresnel formulae are used for the calculation of reflectance at interfaces, and Snell's law for the incidence angles at the subsequent interfaces. Further, we should take into account multiple reflection in one and in multiple slabs (slabs are illuminated by reflected light from the subsequent slab), as indicated in

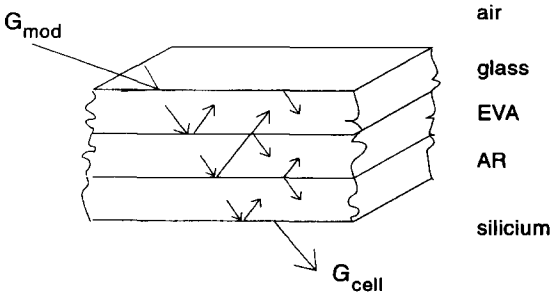

Fig. 2. Three-slab system used to model the PV module cover (not to scale).

Fig. 2. For thin layers (the AR coating) interference may be taken into account by using the matrix method (Hecht, 1987).

Taking into account the reflection and absorption in smooth (non-textured) layers, results in the following formula for two-slabs (Krauter *et al.*, 1994):

$$\tau_{12} = \frac{\tau_1 \tau_2}{T_{12} - (\rho_2 - R_{12})\bar{\rho}_1} \tag{3}$$

The symbols in the formula are explained in the nomenclature at the end of this article. For a three-slab cover the above formula can be applied iteratively, taking the first two slabs together as one:

$$\tau_{123} = \frac{\tau_{12} \tau_3}{T_{23} - (\rho_3 - R_{23})\bar{\rho}_{21}} \tag{4}$$

This formula is slightly different from the one shown in Krauter *et al.* (1994), but ray-tracing confirmed the formula eqn (4) to be more accurate (Kerst, 1995). Even more accurate would be the application of the matrix method for the third (AR) layer, since influence of interference on the absolute transmittance is not negligible in thin layers.

Snell's law of refraction, however, shows that light entering the glass cover layer has an angular distribution within a cone with an opening half-angle of 42°:

$$\Theta \leq 90° \Leftrightarrow \Theta_g = \arcsin(n_g^{-1} \sin \Theta) \leq \arcsin(n_g^{-1}) \tag{5}$$

with Θ_g the angle inside the glass cover layer, and n_g the refractive index of the glass, usually about 1.5 (depending on wavelength and glass type).

This small range of incidence angles at the subsequent interface results in hardly any variation in the transmittance after the air–glass interface. In other words, the transmittance relative to perpendicular incidence is dominated by the air–glass interface. This is illustrated in Fig. 3, where the transmittance relative to STC of the cover layers is shown as a function of incidence angle for unpolarised light and a wavelength of 800 nm (see Sections 2.2 and 2.3 for details). The air–glass model shown only takes into account the reflection at the air–glass interface ($\tau = T_{12}$). We can see that there is hardly any difference between the results from the air–glass model and the detailed three-slab model. For the calculation of the reflection and absorption loss relative to STC the very simple air–glass model may therefore be used instead

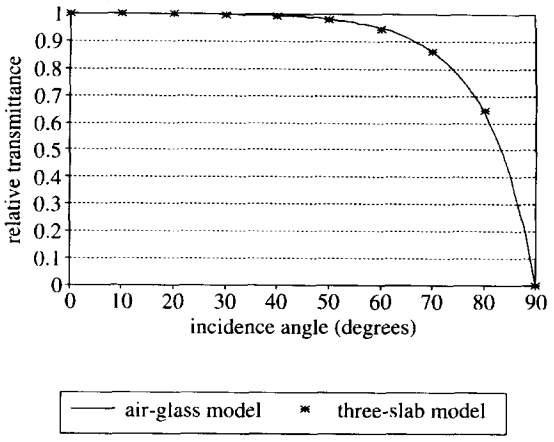

Fig. 3. Transmittance relative to STC as a function of incidence angle according to two models for PV module covers.

of the more elaborate three-slab model or an even more detailed model applying the matrix method.

As a result of the dominance of the air–glass interface, texturing of the *cell* surface is not expected to influence the reflection losses relative to STC significantly. Another conclusion from Fig. 3 is that the reflection losses relative to STC are significant only for incidence angles exceeding 40°. Therefore a minor variation of incidence angles around the perpendicular when measuring the module peak power will hardly influence the STC rating.

2.2. *Dispersion*

The wavelength of the incoming light is a parameter in the calculation of the transmission coefficient. Calculation of the transmittance as a function of incidence angle for different wavelengths within the relevant bandwidth for crystalline Si cells (400–1200 nm) results in Fig. 4,

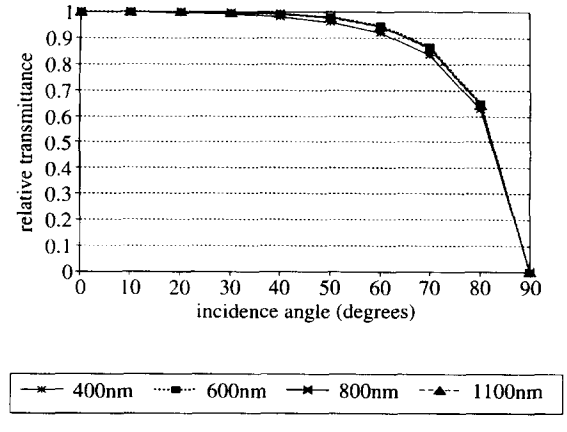

Fig. 4. Transmittance relative to STC as a function of incidence angle for different wavelengths.

for the three-slab model. In this wavelength range the transmittance is hardly influenced by dispersion, a result which is confirmed by measurements (Preu *et al.*, 1995). Therefore we use the curve at 800 nm (which is about the optimum wavelength for crystalline Si cells) for all wavelengths.

2.3. Polarisation

Reflection at the slabs differs for both polarisations, so the transmission coefficient will be influenced by the polarisation of the incoming light. However, the actual polarisation of the irradiance under field conditions is generally not known, and no simple model is available to determine the polarisation. According to Krauter (1993) both direct radiation and radiation reflected by clouds are unpolarised. Von Frisch (1965) reported polarisation values for a specific clear sky situation. Krauter (1993) used these polarisation values to calculate the transmittance of a PV module cover. These calculations result in a transmittance relative to STC of 0.873. Neglecting the polarisation for that situation results in a relative transmittance of 0.926. The polarisation thus results in an "extra" reflection loss of 5% with respect to unpolarised irradiance for this specific situation. Not withstanding the obvious need for research into the polarisation of the incident irradiance, in our model we apply a rough approximation of this "extra" (i.e., with respect to unpolarised irradiance) reflection loss due to polarisation of sky irradiance. We subtract a "polarisation loss", p, from the averaged relative transmittance for the isotropic diffuse irradiance, see Section 3.2. This polarisation loss is approximated as a function of the clearness index K_t, which is the quotient of the global horizontal irradiance and the extra-terrestrial irradiance:

$$K_t = G_h/G_o \tag{6}$$

For clear skies, the polarisation loss equals the previously mentioned 5%, for overcast skies the irradiance is unpolarised. For intermediate values of K_t the polarisation loss is linearly interpolated between 5 and 0%. This results in the following approximation:

$$\begin{aligned} p &= 5\% && K_t \geq 0.75 \\ p &= (K_t - 0.35)\cdot 0.125\% && 0.35 < K_t < 0.75 \\ p &= 0\% && K_t \leq 0.35 \end{aligned} \tag{7}$$

2.4. Other models

In Fig. 5 one sees the transmittance curves relative to STC for the air–glass model and two other models. The air–glass–air model was developed for solar thermal collectors, but sometimes it is erroneously applied to PV modules. Figure 5 shows that the air–glass–air model underestimates the relative transmittance for PV modules.

The third and fourth model shown in Fig. 5 is the ASHRAE model:

$$\tau_{rel}(\Theta) = 1 - b_o(1/\cos\Theta - 1) \tag{8}$$

in which the parameter b_o can be chosen such that a correct representation of the considered optical configuration is obtained. For PV modules a parameter value of $b_o = 0.05$ is claimed to be valid by Schaub *et al.* (1994), whilst for window glass $b_o = 0.1$. The differences between both ASHRAE curves and that of the air–glass model indicate that the value of parameter b_o should be chosen somewhere between these two figures. However, the air–glass model is not more complicated than the ASHRAE model, gives a very good fit to measured data (Preu *et al.*, 1995), and is based on optical formulas without adjustable parameters. Therefore, we recommend using the air–glass model instead of the ASHRAE model as a standard model for practical calculations.

3. AVERAGED REFLECTION LOSS

In this section we present a method to average the relative transmittance presented in Section 2 over the angular distribution of the incident irradiance under field conditions. Calculating the reflection loss over a certain time period

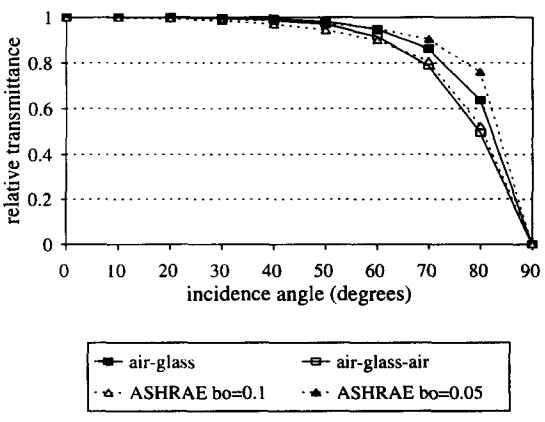

Fig. 5. Transmittance relative to STC as a function of incidence angle according to four models.

(year, month) requires subsequently averaging over that time period.

3.1. *Angular distribution of irradiance*

The transmittance relative to STC, $\tau_{rel}(\Theta)$, has to be averaged over the angular distribution of the incident irradiance at a certain time, in order to calculate the averaged transmission coefficient at that time:

$$\bar{\tau}_{rel}(t) = \frac{\int \tau_{rel}(\Theta) \cdot G(\Theta,t)\, d\Theta}{\int G(\Theta,t)\, d\Theta} \qquad (9)$$

in which $G(\Theta,t)$ is the total irradiance incident with angle Θ at that time.

Here we distinguish five categories of irradiance, for each of which we calculate an averaged transmission coefficient. These five categories are direct, ground-reflected, isotropically diffuse, horizon band diffuse and circumsolar diffuse. We use the Perez model (Perez *et al.*, 1987) as a starting point for the determination of the angular distribution of the irradiance. The Perez model was evaluated as the best model for tilt conversion of diffuse irradiance (van den Brink, 1987; Utrillas and Martinez-Lozano, 1994), and is already used for tilt conversions in our program SOMES (van Dijk and Alsema, 1992). The ground-reflected irradiance is assumed to be distributed isotropically.

For the five categories the averaged relative transmission coefficients are calculated in the following ways.

3.1.1. Direct irradiance. The transmission coefficient for the direct irradiance is calculated directly from the incidence angle, which is calculated using tilt, orientation, location, solar altitude and solar azimuth (Duffie and Beckman, 1991).

3.1.2. Isotropic diffuse, horizon band and ground-reflected irradiance. As the distribution of incidence angles from the isotropic and horizon band diffuse irradiance only depends on the tilt angle of the PV module, their averaged transmission coefficient can be calculated once for every tilt angle. The same is true for isotropic ground-reflected irradiance. For each tilt the (incidence angle dependent) relative transmittance is averaged over the distribution of incidence angles to get the resulting tilt-dependent averaged transmission coefficient:

$$\bar{\tau}_{rel}(\beta) = \frac{\int_{A(\beta)} \tau_{rel}(\Theta)\, d\Omega}{\int_{A(\beta)} d\Omega} \qquad (10)$$

In this formula Θ is the incidence angle on the PV module surface, i.e., at the air–glass interface, and Ω the solid angle of the area to be integrated over. The area A over which the integration is performed depends on the tilt angle β.

For the ground-reflected irradiance the formula is

$$\bar{\tau}_{rel}(\beta) = \frac{2\int_{\phi=0}^{\frac{\pi}{2}} \int_{\Theta=\arctan(\cot\beta/\sin\phi)}^{\frac{\pi}{2}} \tau_{rel}(\Theta)\cos\Theta\sin\Theta\, d\Theta\, d\phi}{\frac{\pi}{2}(1-\cos\beta)} \qquad (11)$$

If we assume the horizon band infinitesimally thin, like in the Perez model, the formula for the horizon band irradiance is

$$\bar{\tau}_{rel}(\beta) = \frac{1}{2}\int_{\phi=0}^{\frac{\pi}{2}} \tau(\arccos[\sin\beta\sin\phi])\sin\phi\, d\phi \qquad (12)$$

For the isotropic sky diffuse irradiance the formula is written as

$$\bar{\tau}_{rel}(\beta) = \frac{\left[2\pi\int_{\Theta=0}^{\frac{\pi}{2}} \tau(\Theta)\cos\Theta\sin\Theta\, d\Theta - 2\int_{\phi=0}^{\frac{\pi}{2}} \int_{\Theta=\arctan(\cot\beta/\sin\phi)}^{\frac{\pi}{2}} \tau(\Theta)\cos\Theta\sin\Theta\, d\Theta\, d\phi\right]}{\frac{\pi}{2}(1+\cos\beta)} - p \qquad (13)$$

where p is the polarisation loss from eqn (7).

The resulting averaged transmission coefficients as a function of the tilt angle are depicted in Fig. 6. In SOMES they are implemented as a look-up table in the source of the simulation program. Thus the calculation in the program

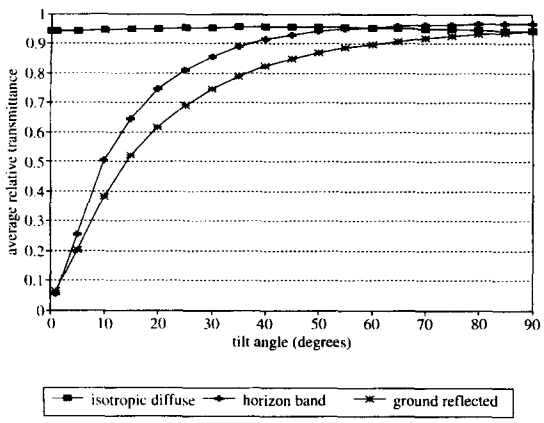

Fig. 6. Tilt dependence of averaged relative transmission coefficient for three categories of irradiance.

itself is reduced to interpolation between the values listed in the table.

3.1.3. Circumsolar diffuse. The circumsolar region is assumed to be small enough so that all points within this region have the same incidence angle, the same assumption as used in the Perez model. The incidence angle for the circumsolar diffuse irradiance is chosen to be equal to the incidence angle of the direct irradiance if all of the circumsolar region (25° half-angle) is "seen" by the array plane. If not, the incidence angle is calculated as a mean value between the point at the largest elevation above the (plane of the array or) horizon and the point at the (array plane) horizon. All circumsolar irradiance is corrected with the relative transmission coefficient for this incidence angle.

The averaged transmission coefficients for the five irradiance categories are multiplied with the irradiance from these categories, which are measured separately or calculated from global horizontal irradiance using (Orgill and Hollands, 1977) and (Perez *et al.*, 1987). Summing over all categories results in the total corrected irradiance available for the solar cell:

$$G_{\text{cell}}(t) \sum_{\text{cat}} \bar{\tau}_{\text{rel,cat}}(t) \cdot G_{\text{mod,cat}}(t) = \bar{\tau}_{\text{rel}}(t) \cdot G_{\text{mod}}(t) \tag{14}$$

In this formula cat indicates the irradiance category (direct, ground-reflected, isotropic diffuse, horizon band diffuse, circumsolar diffuse).

3.2. Time-averaged loss factor

The power reduction caused by reflection and absorption losses relative to the nominal power rating at STC can be calculated over a certain time period, e.g., year, month. These time-averaged losses are referred to as the reflection loss factor $\bar{r}$:

$$\bar{r} = \frac{\int [1 - \bar{\tau}_{\text{rel}}(t)] \cdot G_{\text{mod}}(t)\, \mathrm{d}t}{\int G_{\text{mod}}(t)\, \mathrm{d}t} \tag{15}$$

Note that the loss factor $\bar{r}$ depends on the irradiance incident on the PV module during the averaging period, and thus on array tilt, orientation, location and time.

3.3. Time step dependence of angular distribution

In hourly based simulation models, all irradiance during the hour is usually assumed to be incident with the angles calculated half-way through the hour. This, however, might influence the calculated loss factor. Therefore, in this subsection we compare angular distributions calculated with an hourly time step with those calculated with a 1-min time step.†

In Fig. 7, an angular distribution of yearly global irradiance is shown, calculated with both time steps. The distribution on an hourly basis shows a remarkable peaked structure, whilst the minute-based distribution is much smoother. This peaked structure is found not to depend on the irradiance data but on the frequency distribution of the calculated solar position. The hourly time step in the calculations thus causes an artificial preference for certain incidence angles.

Especially in the steep part of the transmittance curve ($\Theta > 60°$), the error made in the calculation of the incidence angle will lead to a significant difference in the calculated reflection loss. However, the *yearly* reflection losses calculated using the hourly based angular distribution are only about 0.1% smaller than calculated on a minute basis, a difference which is expected to be in the order of magnitude of the accuracy of the $\bar{r}$ model itself. Calculations for the EC Test Reference Years of De Bilt, Lerwick and Cagliari (Lund, 1984), and for the year 1985

†For the calculation on a minute basis, the incidence angles are calculated each minute. The weighting with the irradiance is done assuming the hourly irradiance on the module evenly distributed over the minutes in each hour. The global irradiance incident on the tilted module was calculated on an hourly basis, because the Perez model (Perez *et al.*, 1987) used is based on hourly measurements and may not be accurate when applied on a minute basis (Gansler *et al.*, 1995).

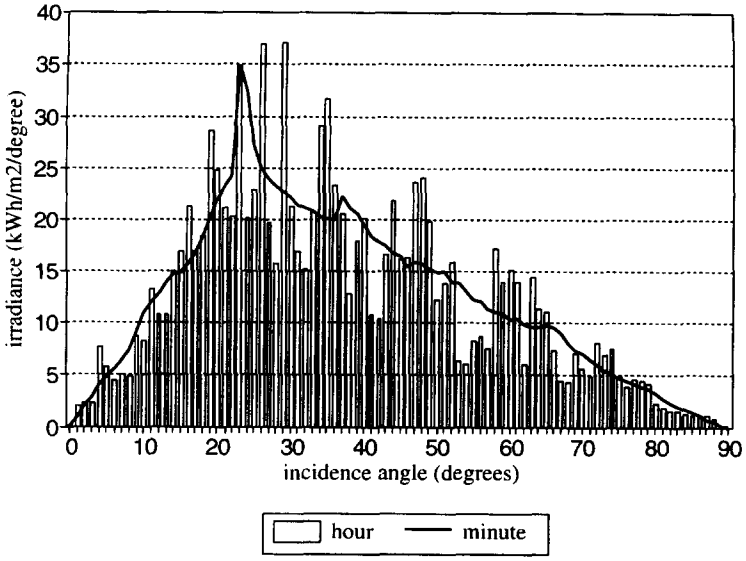

Fig. 7. Angular distribution of the yearly global irradiance on a 52° tilted, south-oriented plane at De Bilt (TRY, 52°N, 5°E). Calculated using hourly and minute time step, respectively.

for Bulawayo, for different tilt angles (see also Section 5.3), showed this difference to be independent of location and tilt. *Monthly* reflection losses for De Bilt show a maximum difference of 0.1% between the two calculation methods. For the EC Test Reference Year at De Bilt, the difference between the *hourly* reflection losses calculated on an hourly and on a minute basis has a mean value of 0.07% and a standard deviation of 0.2%.

Resulting from the inaccuracy in the $\bar{r}$ model induced by the modelling of the incident irradiance as well as the polarisation loss, the more detailed calculations on a minute basis are not considered necessary. We prefer fast and simple modelling for simulation models, and therefore chose the hourly time step already used in SOMES.

4. COMPARISON WITH EXPERIMENTAL DATA

In this section we will try to validate the reflection loss models as discussed in Sections 2 and 3 by comparison with experimental data. We will do this for both the air–glass model for reflection as a function of incidence angle and for the $\bar{r}$ model for estimation of average reflection losses under field conditions.

4.1. Reflection as a function of incidence angle

Preu *et al.* (1995) have performed laboratory measurements on the transmittance of a typical PV module encapsulation which is irradiated with parallel light at varying incidence angles. The resulting curve of the relative transmittance as a function of incidence angle shows very good correspondence with the relative transmittance calculated with the air–glass model discussed in Section 2 (Fig. 3). This means that the air–glass model provides a good basis for the calculation of average module reflection losses in the field.

4.2. Average reflection losses

As discussed in Section 3, the calculation of the average reflection losses expected for a PV module under field conditions involves a second modelling step taking into account the angular distribution of the incident irradiance. We tried to validate the resulting $\bar{r}$ model with experimental data from irradiance measurements performed at our experimental PV system at Utrecht University, The Netherlands. In the array plane (tilt 52°, south oriented) an x-Si reference cell (RSM40) and a pyranometer (Kipp CM11) are mounted. The pyranometer has a flat spectral response, and a semi-spherical glass cover at which light always comes in perpendicularly. In contrast, the reference cell has the same reflection characteristic and spectral response as the PV modules of the system. The reference cell is calibrated at STC.

The relative difference rs between the data measured by the two devices is

$$rs = 1 - (\bar{G}_{\text{reference cell}}/\bar{G}_{\text{pyranometer}}) \quad (16)$$

This difference is caused by (1) the reflection

losses $\bar{r}$ and (2) the spectral losses $\bar{s}$, both relative to STC:

$$rs = \bar{r} + \bar{s} \quad (17)$$

Unfortunately, these two contributions cannot be determined separately from the measured irradiance data. Therefore, to validate our $\bar{r}$ model, we have to estimate the spectral losses.

Nann (1992) has determined monthly and yearly averaged values for the spectral losses at mono-Si modules, using spectral measurements and calculations, for Stuttgart (Germany) over the period of 1987–1989. Combining his spectral loss factors ($\bar{s}$) with our calculated loss factors $\bar{r}$, we obtain model values of the monthly reflection and spectral losses, rs_{model}. In Fig. 8 these model values are shown together with the experimental factors rs_{meas} which are determined from measurement data at Utrecht, using eqn (16).

We can see that the model values are in about the same order of magnitude as the experimental data, particularly on a yearly averaged basis. The difference between experimental and modelled yearly data is 1.2%. It should be noted that unavoidable inaccuracies of the measuring system give a relatively large inaccuracy in the ratio rs_{meas}. Pyranometers for example have 2% inaccuracy on a daily basis (Kipp & Zonen, 1988). Further, an offset error of 1 W m^{-2} may easily be introduced in the measuring chain, and would result in about 0.4% inaccuracy in the yearly average of loss factor rs_{meas}.

Next to these measuring inaccuracies some modelling inaccuracies are present. The large deviation on a monthly basis may well be caused by different spectral losses at Utrecht for the specific month in 1992 with respect to those at Stuttgart over the period 1987–1989.† We recommend further research to be done on spectral effects, aimed at formulating a simple and validated model for the calculation of the spectral losses, i.e., only requiring easily available input parameters.

Another source of errors may be the irradiance models used (Orgill and Hollands, 1977; Perez *et al.*, 1987). Significant deviations were observed between the modelled and measured global irradiance incident on the tilted plane.

†The atmospheric conditions may differ significantly between Utrecht, which is about 100 km from the North Sea, and the more continental climate of Stuttgart. Because data for a location similar to Utrecht are not available, Stuttgart was assumed to give the closest results. A data set with pyranometer and reference cell data like that of Utrecht was not available for Stuttgart.

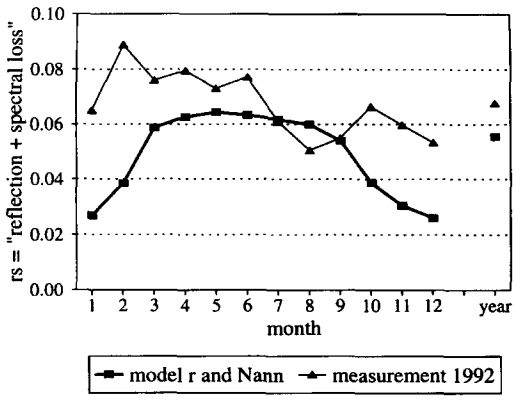

Fig. 8. Combined monthly reflection (r) and spectral (s) loss relative to STC; measurements at Utrecht University and modelled data.

Therefore, validation research on irradiance models for tilt conversions has been planned.

Resulting from the influence of the inaccuracies in the spectral losses and the irradiance model, the $\bar{r}$ model cannot be validated adequately at present. The transmittance curve as a function of incidence angle, however, was confirmed by measurements (Preu *et al.*, 1995). Based on this confirmation and the fair correspondence with our experimental data on a yearly basis, we consider the $\bar{r}$ model to be suitable for the correction of performance calculations in simulation and design of PV systems.

5. SOME SIMULATION RESULTS

In this section we will apply our $\bar{r}$ model to investigate the influence of tilt angle, orientation angle, location, and season on the reflection losses. In this investigation an albedo of 0.2 (grassland) is assumed for the ground-reflected irradiance. At the end of this section the results are compared with results from other models.

5.1. Tilt angle dependence

The incidence angle of the incoming radiation depends on the tilt angle of the PV module. The yearly reflection loss factor as a function of the tilt angle is shown in Fig. 9 for the location of De Bilt (TRY; 52°N, 5°E). The losses are smallest at tilt angles roughly equal to the latitude, explained by the fact that latitude tilt minimises the occurrence of non-perpendicular incidence angles of direct and circumsolar diffuse irradiance.

5.2. Orientation angle dependence

The orientation or azimuth angle of the PV module with respect to a north-facing plane

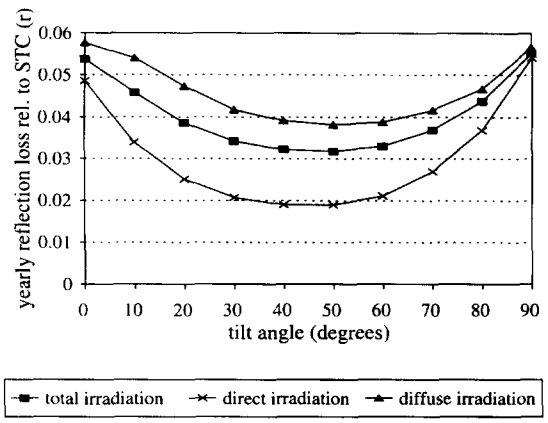

Fig. 9. Yearly reflection loss factor $\bar{r}$ as a function of the tilt angle, for south-oriented modules at De Bilt (TRY, 52°N, 5°E).

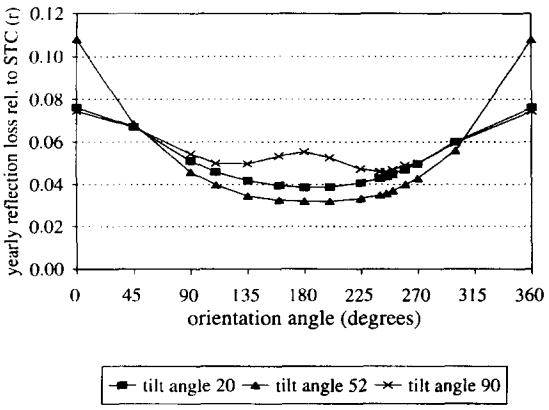

Fig. 10. Yearly reflection loss relative to STC for PV modules at different orientation angles at De Bilt (TRY, 52°N, 5°E).

also has its influence on the distribution of incidence angles. In Fig. 10 the yearly reflection loss factor relative to STC is shown for modules with different tilts at De Bilt.

The influence of orientation angle is significant only for the unusual orientations towards north, northeast and northwest. For vertical modules (facades), the reflection losses at an orientation due south (180°) are slightly larger than at the southeast and southwest orientations. From the angular distributions of yearly global irradiance for modules at Freiburg (Preu *et al.*, 1995), we conclude that the same effect will occur, though this is not reported explicitly. A possible explanation for this effect might be found in different irradiance conditions, especially concerning the amount of diffuse irradiance, between mornings and afternoons. Note, however, that inaccuracies in the used irradiance model might have influenced these results. In future work we plan to investigate this effect in further detail.

5.3. Location dependence

Since the amount of diffuse radiation varies for different climates, the angular distribution of the incoming light and thereby the average reflection losses may differ too. To investigate this effect we use irradiance data for the locations of Lerwick (U.K., 60°N, 1°W), De Bilt (The Netherlands; 52°N, 5°E), Cagliari (Italy; 39°N, 9°E), and Bulawayo (Zimbabwe; 20°S, 29°E). For Lerwick, De Bilt and Cagliari irradiance data from the Test Reference Year are used, for Bulawayo data from 1985 were available. In Fig. 11 the calculated yearly reflection losses at these locations are shown for different tilt angles.

Despite the very different irradiance conditions, the reflection losses for modules with tilt angles equal to the latitude do not show large variations. However, note that large differences in albedos between the locations would result in somewhat larger differences in reflection losses. Note also that tilt angles *not* equal to the latitude show more variation with location, especially in the case of vertically mounted modules. For lower latitudes the difference in angle between the latitude angle, at which the losses are lowest (see Section 5.1), and the vertical tilt angle of 90° is larger. Thus, the yearly reflection loss factor for vertically mounted modules is likely to increase with decreasing latitude. The opposite trend is found for horizontal modules.

5.4. Seasonal dependence

The solar altitude and weather conditions influence the angular distribution of irradiance. We therefore expect the reflection loss factor $\bar{r}$ to have a seasonal variation, which will be smallest near the equator. To investigate this we plotted monthly values for the reflection losses relative to STC for three different tilt angles at De Bilt and Bulawayo in Figs 12 and 13.

The seasonal dependence is significant, especially for the vertically mounted modules. As expected, the seasonal variation is different for both locations. The northern hemisphere has a small solar altitude in winter, resulting in large incidence angles at horizontally mounted modules, and therefore large reflection losses. In summer $\bar{r}$ is largest for vertically mounted modules (facades). At Bulawayo, nearer to the equator, the seasonal variation for modules tilted

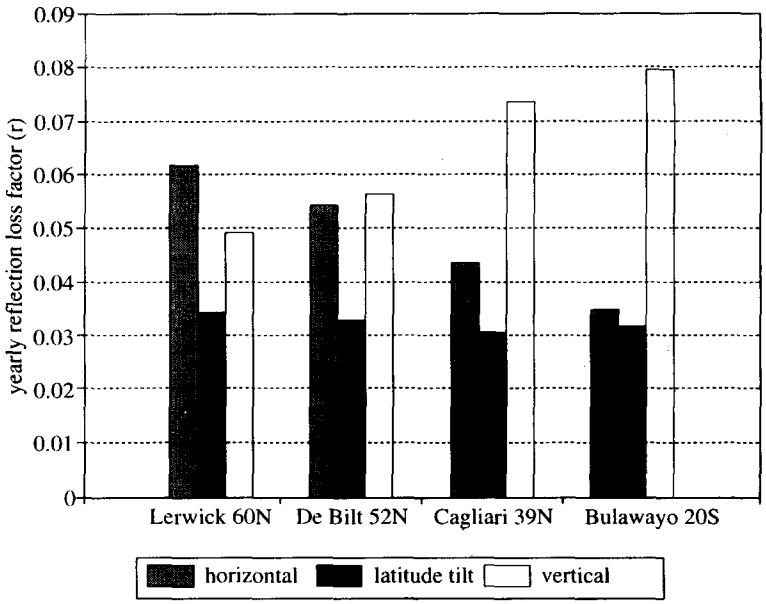

Fig. 11. Yearly reflection loss relative to STC for different locations.

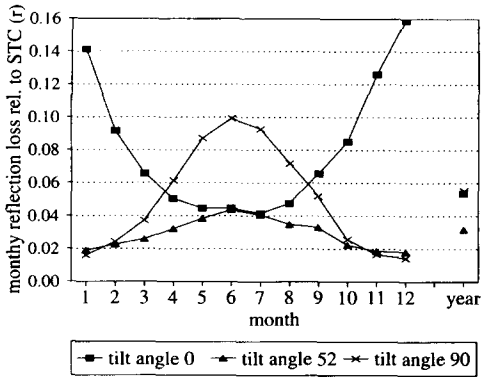

Fig. 12. Monthly reflection loss factors $\bar{r}$ for south-oriented PV modules at De Bilt (TRY, 52°N, 5°E).

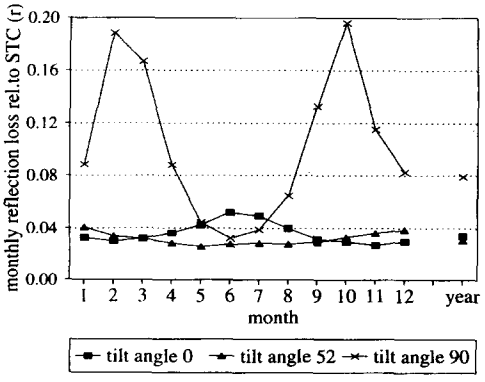

Fig. 13. Monthly reflection loss factors $\bar{r}$ for north-oriented PV modules at Bulawayo (1985, 20°S, 29°E).

with the latitude or mounted horizontally is smaller than at De Bilt, as was expected. However, the seasonal variation of reflection losses at the vertically mounted modules are even larger than at De Bilt. For a vertical module at Bulawayo the maximum reflection losses occur in spring and autumn. This effect is because the Sun is positioned behind the vertical module at Bulawayo during winter, so there is only a contribution from diffuse and ground-reflected irradiance at the front side. In spring and autumn the reflection loss of direct irradiance at the vertical module is larger than that of the diffuse irradiance.

5.5. *Comparison of results with other models*

Our values of about 3% yearly reflection losses at tilt angles equal to the latitude are significantly lower than the 7% reported by Schmid (1993), a value which we cannot explain unless it was calculated for a facade. Even when using the incidence angle of 60° for the diffuse irradiance, as he does, we only get about 4% yearly reflection loss. Preu *et al.* (1995) calculated their values in a way very similar to that which we used (this article and Sjerps-Koomen and Alsema (1995)), but their results are smaller: they report about 2% reflection losses relative to STC for latitude-tilted modules, independent of latitude. Their relative transmission as a function of incidence angle is comparable to the curve used in our calculations. They used a more detailed three-slab model instead of the fast air–glass model we prefer for implementation in simulation models (see Section 2). Preu *et al* (1995), however, do not take polarisation

into account. Assuming unpolarised light in our calculations results in values of about 0.4% less yearly reflection loss.

Another cause for the difference between the results of Preu and ours may be the calculation of the angular distribution. The calculation of the reflection loss relative to STC appears to be sensitive to the irradiance models used and the time step (see Section 3.3) used to calculate the angular distribution of the incident radiation. In future work we plan to show more of the effects of model-dependent distributions. For now the conclusion is that the yearly reflection and absorption losses are most probably in the range of 2–4% for latitude-tilted PV modules. These losses are less than the 5–7% previously reported, but large enough to legitimise the need for adequate modelling in simulation and design studies, especially because of the significant dependence on tilt, orientation, location and season.

6. CONCLUSIONS

The presented model is well suited for the calculation of the seasonal, location and tilt dependence of the reflection losses relative to STC for crystalline Si modules. It can be used in design and simulation of PV systems, to correct the peak power for realistic conditions. Model calculations showed that the air–glass interface determines the reflection losses of a crystalline PV module relative to STC.

Comparison with experimental data, assuming certain spectral losses, resulted in a deviation of 1.2% between the model and experimental data. However, this result depends on the spectral losses assumed and on the model to calculate the angular distribution of the incident irradiance. The use of an hourly versus minute time step was shown not to influence the calculated reflection losses significantly.

Neglecting the reflection losses relative to STC can lead to an overestimation of about 3% of the yearly yield for a PV system tilted with the latitude and oriented towards the equator. This value is only slightly dependent on location. At PV modules in facades the monthly reflection losses show a seasonal variation from 2 to 10% in The Netherlands during the year, and from 3 to 20% at Bulawayo (Zimbabwe).

The results indicate that reflection losses relative to STC, and their seasonal, location, orientation and tilt dependence cannot be neglected.

NOMENCLATURE

G_{cell} irradiance reaching the Si material of the solar cell
G_{mod} irradiance incident on the module front surface
n_g refractive index of glass
R_{ij} reflectance at the interface between slabs i and j
$\bar{r}$ $1-\bar{\tau}_{rel}$, i.e., reflection and absorption loss relative to STC, averaged over a certain time period (hour, month, year)
T_{ij} transmittance of the interface between slabs i and j

Greek letters

β tilt angle of PV module
Θ incidence angle of irradiance on module front surface
Θ_g angle inside the glass cover layer
ρ_i "internal" reflected part of irradiance by slab i when illuminated from the underlying slab
ρ_{ij} idem, for the slab system consisting of slabs i and j
τ transmittance of the material (glass cover, EVA, AR coating, including interfaces) between module front surface and solar cell
τ_{rel} τ relative to the transmission at perpendicular incidence (STC)
$\bar{\tau}_{rel}$ τ_{rel} averaged over the angular distribution of the incident irradiance

Acknowledgement—This work was financially supported by the Netherlands Organisation for Energy and Environment, NOVEM.

REFERENCES

Duffie J. A. and Beckman W. A. (1991) *Solar Engineering of Thermal Processes*, 2nd Edn., pp. 309 and 15. Wiley, New York.

Gansler R. A., Klein S. A. and Beckman W. A. (1995) Investigation of minute solar radiation data. *Solar Energy* **55**, 21–27.

Hecht E. (1987) *Optics*. Addison-Wesley, Reading.

Kerst U. (1995) Personal communication, Nice, 24 October 1995.

Kipp & Zonen (1988) *Instruction Manual Pyranometer CM11*, Part No. 0305-201 (8810). Kipp & Zonen, Delft.

Krauter S. (1993) Betriebsmodell der optischen, thermischen und elektrischen Parameter von photovoltaischen Modulen, Thesis Technischen Universität Berlin. Verlag Köster, Berlin.

Krauter S., Hanitsch R., Campbell P. and Wenham S. R. (1994) Optical modelling, simulation and improvement of PV module encapsulations. In *Proc. 12th Eur. Photovoltaic Solar Energy Conf.*, H.S. Stephens & Associates, Amsterdam, The Netherlands, pp. 1198–1201.

Lund H. (1984) Test Reference Years TRY, CEC R&D Programme Solar Energy, Group F Solar Radiation Data.

Nann S. (1992) Variabilität der spektralen Behstrahlungsstärke der Sonneneinstrahlung und deren Einfluß auf den Wirkungsgrad von Solarzellen, Thesis Universität Oldenburg, Dissertations Druck Darmstadt.

Orgill J. F. and Hollands K. G. T. (1977) Correlation equation for hourly diffuse radiation on a horizontal surface. *Solar Energy* **19**, 357–359.

Perez R., Seals R., Ineichen R., Stewart R. and Menicucci D. (1987) A new simplified version of the Perez diffuse irradiance model for tilted surfaces. *Solar Energy* **39**, 221–231.

Preu R., Kleiss G., Reiche K. and Bücher K. (1995) PV-module reflection losses: measurement, simulation and influence on energy yield and performance ratio. In *Proc. 13th Eur. Photovoltaic Solar Energy Conf.*, Nice, France (in press).

Schaub P., Mermoud A. and Guisan O. (1994) Evaluation of the different losses involved in two photovoltaic sys-

tems. In *Proc. 12th Eur. Photovoltaic Solar Energy Conf.*, Amsterdam, The Netherlands, pp. 859–862.
Scheydecker A., Goetzberger A. and Wittwer V. (1994) Reduction of reflection losses of PV-modules by structured surfaces. *Solar Energy* **53**, 171–176.
Schmid J. (1993) Real energy production of residential photovoltaic systems. In *Proc. 7th Int. Photovoltaic Solar Energy Conf.*, Nagoya, Japan, pp. 359–362.
Sjerps-Koomen E. A. and Alsema E. A. (1995) A model for PV module reflection losses under field conditions. In *Proc. 13th Eur. Photovoltaic Solar Energy Conf.*, Nice, France (in press).
Utrillas M. P. and Martinez-Lozano J. A. (1994) Performance evaluation of several versions of the Perez tilted diffuse irradiance model. *Solar Energy* **53**, 155–162 (and references cited therein).
van den Brink G. J. (1987) Validation of solar radiation models and recommendation of the model for Dutch climatological circumstances, TPD report No. 314.226-3 and 514.015, TPD TNO, Delft.
van Dijk V. A. P. and Alsema E. A. (1992) SOMES version 3.0; Technical Reference Manual. Utrecht University, Utrecht.
von Frisch K. (1965) *Tanzsprache und Orientierung von Bienen*. Springer, Berlin.